Selection and evaluation of different tracking modes performance for parabolic trough solar collector

Mr. Arvind Kumar
MIT, Bulandshahr

Prof. (Dr). Satish Chand
VGI, Greater Noida

Mr. O.P.Umrao
VGI, Greater Noida

Abstract

The tracking and orientation of parabolic trough is very important for efficient performance of collector. In this paper, we have evaluated the performance parameters of PTC such instantaneous efficiency of collector, heat removal factor, solar incident normal to surface, and correction of glass in respect of Local apparent time for the location New Delhi, June 10 . We have also reckoned which tracking is mode suitable in respect economic, operational control tracking system for large solar power generation. We have made program in EES software for entire evaluation and performance graphs.

[1.] Introduction

Parabolic trough solar water heating is one of several well proven solar energy technologies. It is being used on a commercial scale to produce high pressure steam for power generation, as well as on a small scale for commercial and residential applications .The performance of this type of solar collector can be improved greatly by using one of the solar tracking techniques to concentrate a direct solar beam onto the focal point. The tracking technique basically depends on the tracking axis of a solar beam reflector. A comparison of different tracking modes has been thoroughly investigated in the literature. These studies showed that adopting the two-axis solar tracking technique causes the highest increase in system energy output and improves solar energy contribution. Soteris A. Kalogirou [5] provided analysis different collector such optical, thermal and tracking analysis. Duffie et al. [2] delivered depth knowledge solar engineering thermal application. It also provide f-chart design the thermal system Saad D. Odeh et al. [4]presents the design, development, testing and evaluation of an educational single-axis solar tracking parabolic trough collector that represents a standalone system to produce process heat at a moderate temperature for instructional and demonstrative purposes. Hossein Mousazadeh et al. [3] provided the types of sun-tracking systems are reviewed and their cons and pros are discussed. The most efficient and popular sun-tracking device was found to be in the form of polar-axis and azimuth/elevation types. Y. T. Chen et al. [7] investigates the performance of a heliostat field composed of the newly proposed heliostats. In contrast to the dynamic curvature adjustment proposed in our previous work for a solar furnace, a fixed asymmetric curvature is used here with the spinning-elevation tracking method. Chia-Yen Lee et al. [1] providing a high level overview of the sun tracking system field and then describes some of the more significant proposals for closed-loop and open-loop types of sun tracking systems. We have studied the two-axis solar tracking system consumes more energy than the single solar tracking techniques due to the extra control power requirement. Therefore, using the two-axis mode cannot be justified unless the amount of energy produced compensates for the additional elements and maintenance cost.

IJERT

[2.] Parabolic trough collector orientation and tracking modes methodology

PTC is oriented with its focal axis pointed either in the E-W or N-S direction. In the E-W orientation, the focal axis is horizontal, while N-S situation

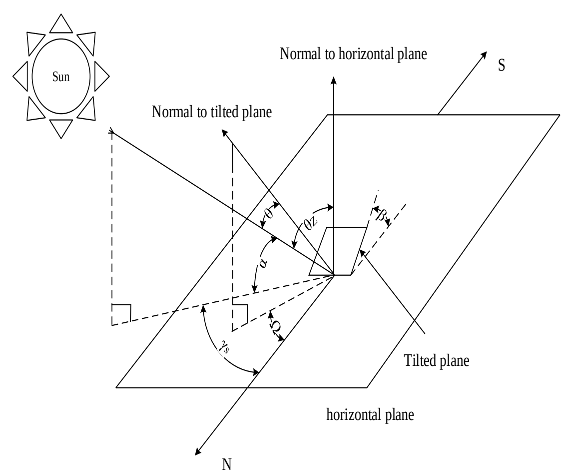

Figure1 this diagram illustrated different angles

, the focal axis may be horizontal or inclined. The following tracking can be adapted, are as follows SP Sukhatme et al [6]

Mode I The focal axis is E-W and horizontal. The collector is rotated about a horizontal E-W axis and adjusted once every day so that the solar beam is normal to the surface of the collector aperture plane at solar noon. The aperture plane is imaginary surface with either $\Omega = 0^0$ or 180^0. The case of $\Omega = 0^0$ happens when (ϕ-δ) <0.then to find the slope β of the aperture plane putting in eq. (1) the condition at the solar noon, viz. $\omega = 0^0$, $\theta = 0^0$. We get

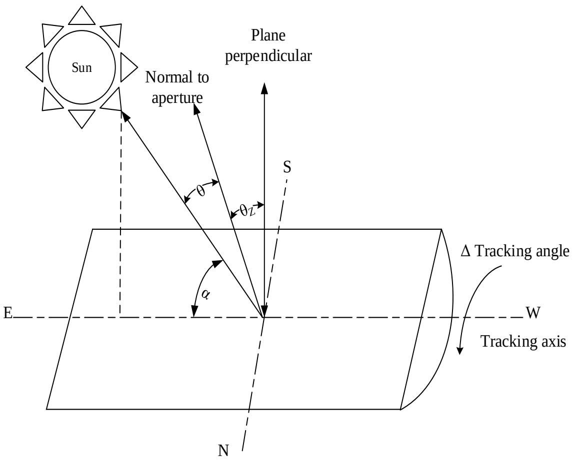

Figure 2 Single axis tracking system rotating about E-W axis

$$\cos\theta = \sin\phi(\sin\delta\cos\beta + \cos\delta\cos\Omega\cos\omega\sin\beta) + \cos\phi(\cos\delta\cos\omega\cos\beta - \sin\delta\cos\Omega\sin\beta) + \cos\delta\sin\Omega\sin\omega\sin\beta \quad (1)$$

$$\beta = (\phi-\delta) \text{ for } \Omega = 0^0 \quad (2)$$

$$\beta = (\phi-\delta) \text{ for } \Omega = 180^0 \quad (3)$$

The angle of indigence of the beam radiation on the aperture plane whole day is obtained by eqs (2) & (3) in eqs (1). For the both cases, $\Omega = 0^0$ or 180^0, we obtain the same relation

$$\cos\theta = \sin^2\delta + \cos^2\delta\ \cos\omega \quad (4)$$

Mode II The focal axis is same as mode I. the collector is turned about the horizontal E-W axis and adjusted continuously so that the solar beam makes the minimum angle of incidence with aperture at all the hours. In order to find the condition to be satisfied for θ to be a minimum, we differentiate the right hand side of the resulting equation with respect to β and equate it to zero.

$$\tan(\phi-\beta) = \frac{\tan\delta}{\cos\omega}\ for\ \ \Omega = 0^0 \quad (5)$$

$$\tan(\phi+\beta) = \frac{\tan\delta}{\cos\omega}\ for\ \ \Omega = 180^0 \quad (6)$$

Above equations can be used for the finding the slope of the aperture plane. Corresponding $\Omega = 0^0$, the magnitude of the solar azimuth angle γ_s is less than 90^0, in respect $\gamma = 180^0$, $\gamma_s > 90^0$

The expression for the minimum angle of incidence is obtained by substituting eqs (3.18) & (3.19), for both cases

$$\cos\theta = (1 - \sin^2\omega\cos^2\delta)^{1/2} \quad (7)$$

Mode III The focal axis is N-S and horizontal. The collector is rotated about a horizontal N-S axis and adjusted continuously so that the solar beam makes the minimum angle of incidence with aperture at all the times. In this mode, surface azimuth angle Ω = +90 before noon and Ω = -90 after noon. The before noon equation becomes

$$\cos\theta = [(\sin\phi\sin\delta + \cos\phi\cos\delta\cos\omega)^2 + \cos^2\delta\sin^2\omega)]^{\frac{1}{2}} \quad (8)$$

$$\beta = \tan^{-1}\left[\frac{\cos\delta\sin\omega}{\sin\phi\sin\delta + \cos\phi\cos\delta\cos\omega}\right] \quad (9)$$

This is used to find the slope of the aperture plane at any hours before noon. The equation for the corresponding minimum angle of the incidence is obtained by putting, giving

$$\cos\theta = [(\sin\phi\sin\delta + \cos\phi\cos\delta\cos\omega)^2 + \cos^2\delta\sin^2\omega)]^{1/2}$$

After noon $\Omega = -90^0$, we have

$$\beta = \tan^{-1}\left[\frac{-\cos\delta\sin\omega}{\sin\phi\sin\delta + \cos\phi\cos\delta\cos\omega}\right] \quad (10)$$

The expression for cosθ remains same.

Mode IV the line of receiver is N-S and inclined at a fixed angle equal to the latitude Thus, it is parallel to the earth's axis. This orientation is sometimes referred to as a polar mount. The collector is rotated about an axis parallel to the earth's axis at an angular velocity equal and opposite to the earth's rate of the rotation (15^0 per hour). It is adjusted such that at solar noon the aperture plane is inclined surface facing due south. Thus, putting β=ϕ and ω=0 in eqs (1), we get

$$\theta = \delta \quad (11)$$

Mode V The focal axis is N-S and inclined. The collector is rotated continuously(but not at a constant angular velocity) about an axis parallel to the focal axis, as well as about a horizontal axis perpendicular to

IJERT

this axis and adjusted so that the solar beam is normally inclined on the aperture plane at all the times. In this situation cosθ =1, it is easy to show that at solar noon

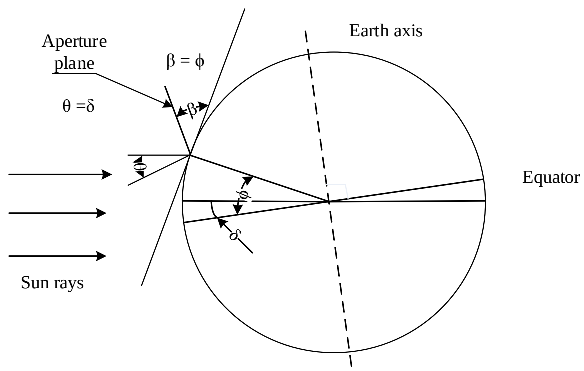

Figure 3 for Cylindrical parabolic collector where θ=δ

$$\beta = |\phi - \delta| \qquad (12)$$

It is of interest to compare the amount of the beam radiation which would be incident on the collector aperture plane over a day if one adopted the various tracking modes.

[3.] Performance of different modes of tracking with graphs

The Location is New Delhi (28.58^0 N, 77.20^0 E); the radiation falls on one square meter of the aperture plane of the collector from 0600 to 1800 h (LAT) on June 10. The following value of S is given in table then we have compared performance of tracking mode which is applicable for requirement. I have made program by EES software for this condition. By this program code prepared graphs between important parameters. In this paper, we have shown all equation in program section 4 avoid the paper space and time.

Table 1 Solar radiation incident data on 10 June, New Delhi from 6.30 am to 5.30 pm

Time (h)	S (W/m^2)	Time (h)	S (W/m^2)
0630	110	1230	523
0730	240	1330	495
0830	333	1430	445
0930	424	1530	322
1030	495	1630	220
1130	550	1730	118

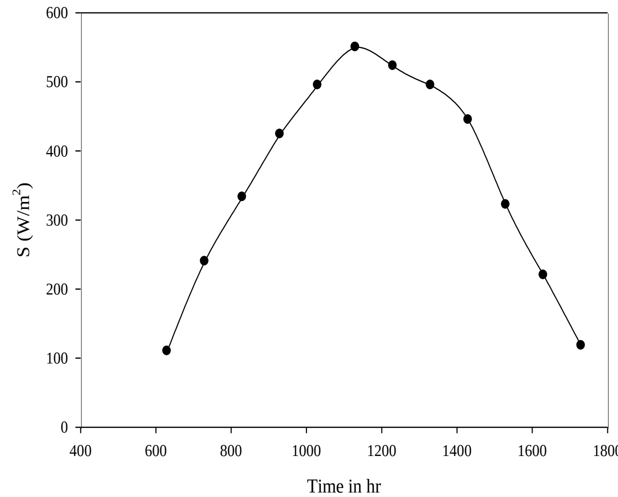

Figure 4 Incident radiation versus LAT

[4.] EES software codes for evaluation tracking modes

"This program code is prepared for EES software. There are five tracking mode and orientation. This program is evaluated which tracking mode is best for New Delhi location for June 10, by comparing data such incident flux, heat removal factor, collector efficiency factor ,instantaneous efficiency of collector from time 0600 to 1500 hrs. . I have plotted number of graphs to check the performance particular time of day"

```
"Orientation and tracking mode"
d=a*60;
LAT=(a+b)*100 [Hrs.]
Min=d+b*100;
IST=720
omega=(IST-Min)/4
delta=23.45*sin((360/365)*(284+n))"declination in degree"
"For horizontal surface beta = 0 degree"
theta_z=arccos(sin(phi)*sin(delta)+cos(phi)*cos(delta)*cos(omega))
"According tracking mode I"
theta_mode1=arccos((sin(delta)^2+cos(delta)^2*cos(omega)))
"According tracking mode II"
theta_mode2=arccos((1-sin(omega)^2*cos(delta)^2)^(1/2))
"According tracking mode III"
beta=arctan((cos(delta)*sin(omega))/(sin(phi)*sin(delta)+cos(phi)*cos(delta)*cos(omega)))
theta_mode3=arccos((sin(phi)*sin(delta)+cos(phi)*cos(delta)*cos(omega))*cos(beta)+cos(delta)*sin(omega)*sin(beta))
"According tracking mode IV"
```

IJERT

```
theta_mode4=delta
"According tracking mode V"
theta_mode5=0
"Tilt factor r_b for the aperture plane"
r_b1=cos(theta_mode1)/cos(theta_z)
r_b2=cos(theta_mode2)/cos(theta_z)
r_b3=cos(theta_mode3)/cos(theta_z)
r_b4=cos(theta_mode4)/cos(theta_z)
r_b5=cos(theta_mode5)/cos(theta_z)
"Beam flux incident normally on aperture plane"
S_mode1=I_b*r_b1
S_mode2=I_b*r_b2
S_mode3=I_b*r_b3
S_mode4=I_b*r_b4
S_mode5=I_b*r_b5
"Absorbed flux S"
tau=0.89;     alfa=0.94;     rho=0.94;     gamma=0.94;
D_o=0.07 [meter]; W_a=5.76 [meter]
S_1=S_mode1*tau*alfa*(rho*gamma+(D_o)/(W_a-D_o))
S_2=S_mode2*tau*alfa*(rho*gamma+(D_o)/(W_a-D_o))
S_3=S_mode3*tau*alfa*(rho*gamma+(D_o)/(W_a-D_o))
S_4=S_mode4*tau*alfa*(rho*gamma+(D_o)/(W_a-D_o))
S_5=S_mode5*tau*alfa*(rho*gamma+(D_o)/(W_a-D_o))
"Inside convective the heat transfer coefficient for receiver tube"
D_i=.055 [meter];
L=98.5 [meter];
A_r=3.14*D_i*L
"Receiver area"
m_steam=1.11 [Kg/sec]
 mu_water=.000128 [Kg/ms]
c_p=4800 [J/kgK]
 k_f=.622 [KW/mK];
K=20.2 [W/mK]
U_L=20.46 [W/(m^2*K)];
D_g=0.1[meter]
R_e=4*m_steam/(3.14*D_i*mu_water)
 "Renold number"
P_r=(c_p*mu_water)/(k_f)   "Prandtl number"
N_u=0.23*(R_e)^(0.8)*(P_r)^(0.4) "Nusselt number"
h_fi=(N_u*k_f)/D_i "Inside heat transfer coefficient"
F=(1/U_L)/((1/U_L)+((D_o)/(h_fi*D_i))+D_i/(2*K)*ln(D_o/D_i))   "Collector efficiency factor"
F_R=(m_steam*c_p)/(A_r*U_L)*(1-exp(-(U_L*F*A_r)/(m_steam*c_p)))"Heat removal factor"
"Useful heat gain rate"
T_i=100 [^0C]; T_a=35 [^0C]
C=(W_a-D_o)/(3.14*D_o)
Q_U1=F_R*(W_a-D_o)*L*(S_1-U_L*(T_i-T_a)/C)
"Mode I"
Q_U2=F_R*(W_a-D_o)*L*(S_2-U_L*(T_i-T_a)/C)
"Mode II"
Q_U3=F_R*(W_a-D_o)*L*(S_3-U_L*(T_i-T_a)/C)
"Mode III"
Q_U4=F_R*(W_a-D_o)*L*(S_4-U_L*(T_i-T_a)/C)
"Mode IV"
Q_U5=F_R*(W_a-D_o)*L*(S_5-U_L*(T_i-T_a)/C)
"Mode V"
"The rate of heat loss"
Q_1=(W_a-D_o)*L*S_1-Q_U1
P_1=3.14*D_o*L*U_L*(T_m1-T_a)
Q_1=P_1
Q_2=(W_a-D_o)*L*S_2-Q_U2
P_2=3.14*D_o*L*U_L*(T_m2-T_a)
Q_2=P_2
Q_3=(W_a-D_o)*L*S_3-Q_U3
P_3=3.14*D_o*L*U_L*(T_m3-T_a)
Q_3=P_3
Q_4=(W_a-D_o)*L*S_4-Q_U4
P_4=3.14*D_o*L*U_L*(T_m4-T_a)
Q_4=P_4
Q_5=(W_a-D_o)*L*S_5-Q_U5
P_5=3.14*D_o*L*U_L*(T_m5-T_a)
Q_5=P_5
"Overall heat transfer coefficient for wind"
rho_air=1.105 [Kg/m^3]
v_air=3.01 [m^2/s]
mu_air=.0000205 [Kg/ms]
k_air=0.028 [W/mK]
Re_air=rho_air*v_air*D_g/mu_air
N_u_air=0.3*(Re_air)^(0.6)
h_w=N_u_air*k_air/D_g
b_a=(D_g-D_o)/2

"Heat transfer coefficient between the absorber tube and cover evaluated by Raithby and Holland"
"The properties are based on the mean temperature between tube and glass cover"
k_a= 0.0323 [W/mK];
nu_a=23.52*10^ (-6)
pr_a=0.688
T_guess=30 [^0C]
T_ra1=(T_m1+T_guess+273+273)/2
"Mean Temperature of air between tube and cover"
T_ra2=(T_m2+T_guess+273+273)/2
T_ra3=(T_m3+T_guess+273+273)/2
T_ra4=(T_m4+T_guess+273+273)/2
T_ra5=(T_m5+T_guess+273+273)/2
Ra_1=9.81*(T_ra1)^(-1)*(T_m1-T_guess)*b_a^3*pr_a/(nu_a)^2
Ra_star1=ln(D_g/D_o)*(Ra_1)^(1/4)*(b_a)^(-3/4)/(D_o^(-3/5)+(D_g)^(-3/5))^(5/4)
K_eff1/k_a=0.317*(Ra_star1)^(1/4)
h_c_1= (2*k_eff1)/ (D_o*ln(D_g/D_o))
```

IJERT

```
Ra_2=9.81*(T_ra2)^(-1)*(T_m2-T_guess)*b_a^3*pr_a/(nu_a)^2  " Rayleigh number "
Ra_star2=ln(D_g/D_o)*(Ra_2)^(1/4)*(b_a)^(-3/4)/(D_o^(-3/5)+(D_g)^(-3/5))^(5/4)   "Modified Rayleigh number related to the usual Rayleigh number "
K_eff2/k_a=0.317*(Ra_star2)^(1/4)   "Effective thermal conductivity"
h_c_2= (2*k_eff2)/(D_o*ln(D_g/D_o))
Ra_3=9.81*(T_ra3)^(-1)*(T_m3-T_guess)*b_a^3*pr_a/(nu_a)^2
Ra_star3=ln(D_g/D_o)*(Ra_3)^(1/4)*(b_a)^(-3/4)/(D_o^(-3/5)+(D_g)^(-3/5))^(5/4)
K_eff3/k_a=0.317*(Ra_star3) ^(1/4)
h_c_3= (2*k_eff3)/(D_o*ln(D_g/D_o))
Ra_4=9.81*(T_ra4)^(-1)*(T_m4-T_guess)*b_a^3*pr_a/(nu_a)^2
Ra_star4=ln(D_g/D_o)*(Ra_4)^(1/4)*(b_a)^(-3/4)/(D_o^(-3/5)+(D_g)^(-3/5))^(5/4)
K_eff4/k_a=0.317*(Ra_star4) ^ (1/4)
h_c_4= (2*k_eff4)/(D_o*ln(D_g/D_o))
Ra_5=9.81*(T_ra5)^(-1)*(T_m5-T_guess)*b_a^3*pr_a/(nu_a)^2
Ra_star5=ln(D_g/D_o)*(Ra_5)^(1/4)*(b_a)^(-3/4)/(D_o^(-3/5)+(D_g)^(-3/5))^(5/4)
K_eff5/k_a=0.317*(Ra_star5)^(1/4)
h_c_5= (2*k_eff5)/(D_o*ln(D_g/D_o))
"General Correlation of energy"
sigma=5.70*10^(-8); epsilon_r=0.93
epsilon_g=0.88; T_sky=30 [^0C]
x_1=h_c_1*(T_m1-T_g1)*3.14*D_o+sigma*3.14*D_o/(1/epsilon_r+D_o*(D_g)^(-1)*(1/epsilon_g-1))*((T_m1+273)^4-(T_g1+273)^4)
y_1=h_w*(T_g1-T_a)*3.14*D_g+sigma*3.14*D_g*epsilon_g*((T_g1+273)^4-(T_sky+273)^4)
x_1=y_1
x_2=h_c_2*(T_m2-T_g2)*3.14*D_o+sigma*3.14*D_o/(1/epsilon_r+D_o*(D_g)^(-1)*(1/epsilon_g-1))*((T_m2+273)^4-(T_g2+273)^4)
y_2=h_w*(T_g2-T_a)*3.14*D_g+sigma*3.14*D_g*epsilon_g*((T_g2+273)^4-(T_sky+273)^4)
x_2=y_2
x_3=h_c_3*(T_m3-T_g3)*3.14*D_o+sigma*3.14*D_o/(1/epsilon_r+D_o*(D_g)^(-1)*(1/epsilon_g-1))*((T_m3+273)^4-(T_g3+273)^4)
y_3=h_w*(T_g3-T_a)*3.14*D_g+sigma*3.14*D_g*epsilon_g*((T_g3+273)^4-(T_sky+273)^4)
x_3=y_3
x_4=h_c_4*(T_m4-T_g4)*3.14*D_o+sigma*3.14*D_o/(1/epsilon_r+D_o*(D_g)^(-1)*(1/epsilon_g-1))*((T_m4+273)^4-(T_g4+273)^4)
y_4=h_w*(T_g4-T_a)*3.14*D_g+sigma*3.14*D_g*epsilon_g*((T_g4+273)^4-(T_sky+273)^4)
x_4=y_4
x_5=h_c_5*(T_m5-T_g4)*3.14*D_o+sigma*3.14*D_o/(1/epsilon_r+D_o*(D_g)^(-1)*(1/epsilon_g-1))*((T_m5+273)^4-(T_g5+273)^4)
y_5=h_w*(T_g5-T_a)*3.14*D_g+sigma*3.14*D_g*epsilon_g*((T_g5+273)^4-(T_sky+273)^4)
x_5=y_5

"Correction of overall heat transfer coefficient"
U_correct1=x_1/ (3.14*D_o*(T_m1-315.1))
U_correct2=x_2/ (3.14*D_o*(T_m2-315.1))
U_correct3=x_3/ (3.14*D_o*(T_m3-315.1))
U_correct4=x_4/ (3.14*D_o*(T_m4-315.1))
U_correct5=x_5/ (3.14*D_o*(T_m5-315.1))

"Exit temperature of steam going to steam turbine"
c_po=4800[J/kgK]
m_steam*c_po*(T_fo1-100) =Q_U1/1000
m_steam*c_po*(T_fo2-100) =Q_U2/1000
m_steam*c_po*(T_fo3-100) =Q_U3/1000
m_steam*c_po*(T_fo4-100) =Q_U4/1000
m_steam*c_po*(T_fo5-100) =Q_U5/1000

"Instantaneous efficiency"
eta_i1=Q_U1/ (S_mode1*W_a*L)
eta_i2=Q_U2/ (S_mode2*W_a*L)
eta_i3=Q_U3/ (S_mode3*W_a*L)
eta_i4=Q_U4/ (S_mode4*W_a*L)
eta_i5=Q_U5/ (S_mode5*W_a*L)
```

IJERT

Table 2. Calculated results of solar radiation flux for different tracking modes during LAT by EES software

LAT	ω	S_{mode1}	S_{mode2}	S_{mode3}	S_{mode4}	S_{mode5}
630	82.5	99	154	360	346	376
730	67.5	231	254	476	445	484
830	52.5	328	335	489	451	490
930	37.5	422	424	512	471	512
1030	22.5	496	496	529	488	530
1130	7.5	552	552	554	512	557
1230	-7.5	525	525	527	487	529
1330	-22.5	496	496	529	488	530
1430	-37.5	443	445	537	495	537
1530	-52.5	317	324	473	437	474

ISSN: 2278-0181
Vol. 2 Issue 6, June - 2013

Table 3.Calculated results of collector efficiency for different tracking modes during LAT by EES software

LAT	θ_z	η_{i1}	η_{i2}	η_{i3}	η_{i4}	η_{i5}
630	73	0.22	0.39	0.576	0.57	0.582
730	60.2	0.5	0.52	0.609	0.6	0.611
830	47.2	0.56	0.57	0.612	0.6	0.612
930	34.1	0.6	0.6	0.616	0.61	0.616
1030	21	0.61	0.61	0.62	0.61	0.62
1130	8.75	0.62	0.62	0.624	0.62	0.624
1230	8.75	0.62	0.62	0.619	0.61	0.62
1330	21	0.61	0.61	0.62	0.61	0.62
1430	34.1	0.6	0.6	0.621	0.61	0.621
1530	47.2	0.56	0.56	0.6	0.6	0.609

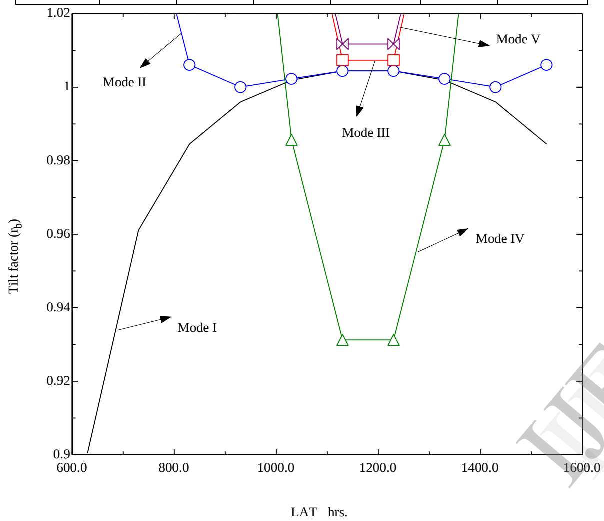

Figure 5 Tilt factor versus local apparent time

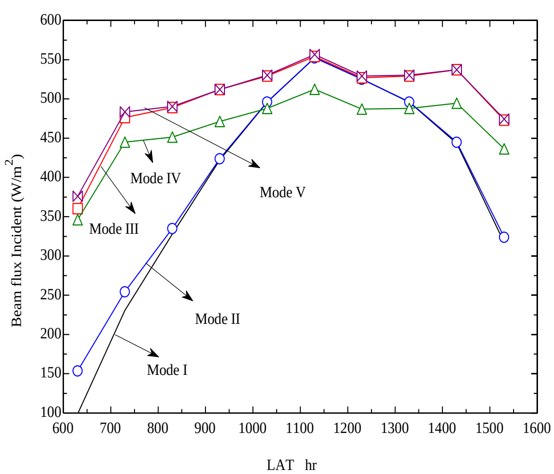

Figure 6 Beam flux incident versus LAT hr. for June 10

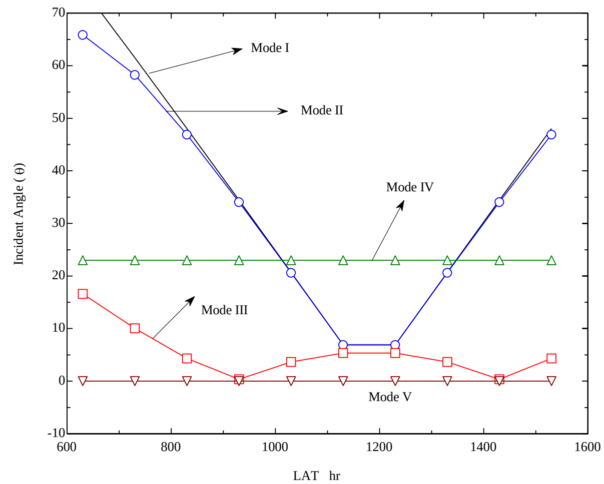

Figure 7 Incident angle versus LAT hr. June 10

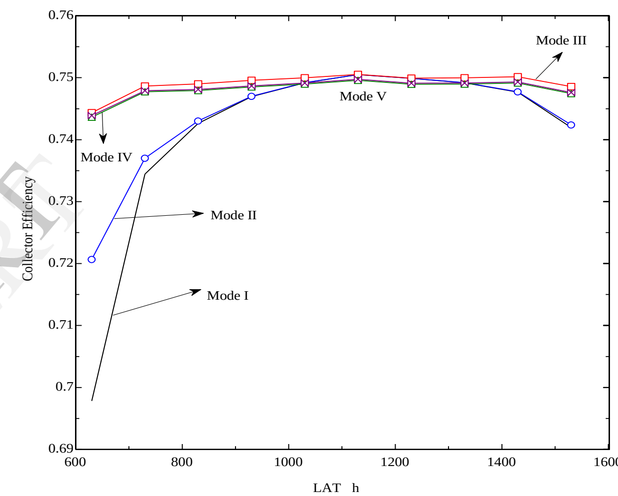

Figure 8 Collector efficiency versus Local Apparent time in hr. June 10

[5.]Conclusion

We observed from the graph and tabular data that shows Collector efficiency, Mode V>Mode III>Mode IV>Mode II >Mode I.

- Mode V is highest efficiency but it is complicated operational control three axis and costly but we can be used for small scale power generation.
- Mode IV is not economic for power generation because lesser efficiency as compared Mode III
- Mode III and Mode II is the best tracking mode for large scale power generation.
- Mode I is lowest efficiency thus it can be used for heating water and cooling purpose not for power generation.

IJERT

Nomenclature

A_a	Aperture area of the collector, [m^2]
A_r	area of the receiver, [m^2]
c_{pw}	Specific heat of water, [J/kg.K]
c_{pa}	Specific heat of air at T_a , [J/kg.K]
D_o	outer diameter of receiver tube [m]
D_i	Inner diameter of receiver tube [m]
T_r	Receiver temperature [K]
F_R	Collector heat-removal factor
S	Direct normal (beam) irradiance, [W/m^2]
h_{fi}	Heat transfer coefficient inside the pipe,[W/m^2.K]
Kss	Stainless steel Thermal conductivity of pipe, [W/m.K]
K_f	Thermal conductivity of water, [W/m.K]
K_{air}	Thermal conductivity of air , [W/m.K]
M_{steam}	Mass flow rate of the steam [kg/s]
F'	Collector efficiency factor
h_w	loss coefficient for wind
Tg	Glass cover temperature,[K]
D_g	Diameter of glass cover ,[m]
D_r	Diameter of receiver ,[m]
n	Day number
Q_U	Solar collector useful output, [W/m^2]
To	Heat transfer fluid outlet (from the collector) temperature, [K]
Ti	inlet temperature of fluid in the collector, [K]
Ta	Ambient temperature, [K]
T_m	Mean temperature of the heat transfer fluid across the collector or the solar field, [K]
V	Wind speed, [m/s]
U_L	Overall heat loss coefficient from absorber surface, [W/m^2.K]
Wa	Collector width, [m]

Dimensionless groups

Nu	Nusselt number
Pr	Prandtl number
Ra	Rayleigh number
Re	Reynolds number

Greek symbols

η_i	Instantaneous efficiency
ε	Emissivity coefficient
ρ_w	Density of water, [kg/m^3]
ρ	Reflectivity constant
τ	Transmittance of the receiver glass envelope
α	Solar altitude angle
α_c	Absorptance of the absorber surface coating
γ	Intercept factor
μ_{water}	Dynamic viscosity of water, [N.s/m^2]
μ_{air}	Dynamic viscosity of air, [N.s/m^2]

References

[1.] Chia-Yen Lee, Po-Cheng Chou, Che-Ming Chiang and Chiu-Feng Lin, Sun Tracking Systems: A Review sensors ISSN 1424-8220

[2.] Duffie; J. A.; Beckman, W. A.: Solar Engineering of Thermal Processes; John Wiley & Sons, New York, Brisbane, USA, 1991, 2nd edition

[3.] Hossein Mousazadeh, Alireza Keyhani, Arzhang Javadi, Hossein Mobli, Karen Abrinia, Ahmad Sharifi, Renewable and Sustainable Energy Reviews 13 (2009) 1800–1818

[4.] Saad D. Odeh & Hosni I. Abu-Mulaweh, Design and development of an educational solar tracking parabolic trough collector system, Global Journal of Engineering Education, Volume 15, Number 1, 2013

[5.] Soteris A. Kalogirou, Solar Energy Engineering Processes and Systems, Academic Press is an imprint of Elsevier

[6.] SP Sukhatme, JK Nayak, Solar energy: Principles of thermal collection and storage Page no.206, Mc raw Hill

[7.] Y. T. Chen, A. Kribus, B. H. Lim, C. S. Lim, K. K. Chong, J. Karni, R. Buck, A. Pfahl and T. P. Bligh Comparison of Two Sun Tracking Methods in the Application of a Heliostat Field ,Journal of Solar Energy Engineering ,Volume 126 ASME,124:98

IJERT